**Jean-François Deü**[1]
Professor
Structural Mechanics and Coupled Systems Laboratory,
Conservatoire National des Arts et Métiers,
2 rue Conté,
Paris 75003, France
e-mail: jean-francois.deu@cnam.fr

**Walid Larbi**
Assistant Professor
Structural Mechanics and Coupled Systems Laboratory,
Conservatoire National des Arts et Métiers,
2 rue Conté,
Paris 75003, France
e-mail: walid.larbi@cnam.fr

**Roger Ohayon**
Professor
Fellow ASME
Structural Mechanics and Coupled Systems Laboratory,
Conservatoire National des Arts et Métiers,
2 rue Conté,
Paris 75003, France
e-mail: roger.ohayon@cnam.fr

**Rubens Sampaio**
Professor
Mechanical Engineering Department,
PUC-Rio,
Rua Marques de Sao Vicente, 225 Gavea,
Rio de Janeiro, RJ 22453-900, Brazil
e-mail: rsampaio@puc-rio.br

# Piezoelectric Shunt Vibration Damping of Structural-Acoustic Systems: Finite Element Formulation and Reduced-Order Model

*For noise and vibration attenuation, various approaches can be employed depending on the frequency range to attenuate. Generally, active or passive piezoelectric techniques are effective in the low-frequency range, while dissipative materials, such as viscoelastic or porous treatments, are efficient for higher-frequency domain. In this work, a reduced-order model is developed for the approximation of a fully coupled electromechanical-acoustic system using modal projection techniques. The problem consists of an elastic structure with surface-mounted piezoelectric patches coupled with a compressible inviscid fluid. The piezoelectric elements, connected with resonant shunt circuits, are used for the vibration damping of the coupled system. Numerical examples are presented in order to illustrate the accuracy and the versatility of the proposed reduced-order model, especially in terms of prediction of attenuation.* [DOI: 10.1115/1.4027133]

## 1 Introduction

Over the past decade, a considerable amount of research has been devoted to the development, testing, and modeling of noise and vibration reduction techniques using passive and/or active approaches. Classically, passive techniques are achieved by using dissipative materials, such as viscoelastic treatments or porous insulations. It is well known that these kinds of methods are quite effective at high frequencies. In the low-frequency range, techniques using piezoelectric materials are found to be an attractive alternative or complementary tool. In this case, sensor and actuator piezoelectric patches are surface-mounted or embedded in the structure. These patches are capable of self-sensing and self-actuation for active vibration and noise control [1,2]. For the numerical modeling of active-control structural-acoustic problems in the field of noise reduction applications, the finite element method is one of most powerful approaches. In this context, let us mention Refs. [3] and [4], where active controller designs are developed to reduce interior cabin noise levels, and Ref. [5], where active/passive constrained layer damping treatments are proposed to control sound radiation from a vibrating thin structure into an acoustic cavity. Another numerical methodology consists of combining the finite element approach for the smart structure and the boundary element method to calculate the acoustic response of the enclosed fluid. In such a case, a steady-state response of acoustic cavities bounded by piezoelectric composite shell structures is proposed in Ref. [6], and an active-passive control technique, based on an output feedback optimal controller design, is developed in Ref. [7]. Other smart systems consist of connecting the piezoelectric elements to a passive electrical circuit, called shunts, which is another way to dissipate the mechanical energy (see for example Refs. [8]–[10]). We only consider in the present work resonant shunt circuits (RL-shunt), which are known to be very efficient to attenuate the vibration level at the resonances, although they present the drawbacks of requiring large inductor value and precise tuning. These drawbacks can be avoided by using electrical synthetic components (requiring an external electric power) and/or using semipassive devices, such as synchronized switch techniques [10]. These two points have been discarded here, but the computational models developed in this work can be adapted to treat numerically such configurations. In the present paper, we consider a physical system constituted of an elastic structure with shunted surface-mounted piezoelectric patches coupled with a linear homogeneous acoustic fluid. The piezoelectric elements, connected with RL-shunt circuits, are used for the vibration damping of the fluid-structure system in the low-frequency range. Such a type of problem has been already analyzed by the authors using the finite element method based on an original fully coupled electromechanical-acoustic formulation [11]. For multiphysics complex systems, the use of direct finite element methods can lead to a huge number of degrees-of-freedom and consequently to a prohibitive cost of the simulations, especially for sensitivity and optimization analyses. The challenge is therefore to construct an

[1]Corresponding author.

Contributed by the Design Engineering Division of ASME for publication in the Journal of Vibration and Acoustics. Manuscript received August 29, 2012; final manuscript received March 1, 2014; published online April 1, 2014. Assoc. Editor: Jiong Tang.

  

appropriate reduced-order model of the multiphysics coupled system. Let us recall that, for structural-acoustic interior vibration problems, without any piezoelectric treatment, various reduced-order models have been widely discussed in literature. These models depend of the initial variational formulation and the corresponding unknown fields. For the fluid, the chosen variables can be the displacement, the pressure, or the displacement or velocity potential, leading to various symmetric or nonsymmetric formulations [12–17]. The objective here is to derive an appropriate reduced-order model for the fluid/structure/piezopatches coupled system.

The outline of the paper is as follows. Firstly, we briefly recall the finite element discretization of the coupled system derived from a multifield variational principle involving structural displacement, electrical voltage of piezoelectric elements, and acoustic pressure inside the fluid cavity [11]. This formulation, with only a couple of electric variables per patch, is well adapted to practical applications, since realistic electrical boundary conditions, such that equipotentiality on the electrodes and prescribed global electric charges, naturally appear. The global charge/voltage variables are intrinsically adapted to include any external electrical circuit into the electromechanical problem and to simulate the effect of resistive or resonant shunt-damping techniques. Then, we develop an appropriate reduced-order model of the coupled problem. This constitutes the main originality of the paper. The proposed methodology, based on a normal mode expansion, requires the computation of the eigenmodes of the structure in vacuo with short-circuited piezoelectric patches and those of the rigid acoustic cavity. It is shown that the projection of the full-order coupled finite element model on the uncoupled bases leads to a reduced-order model in which the main parameters are the classical fluid-structure and electromechanical modal coupling factors. Despite its reduced size, this model is proven to be very efficient for simulations of harmonic vibration analyses of the coupled structural-acoustic system with shunt damping. In the last part of the paper, a three-dimensional numerical example is investigated. The problem consists of an elastic plate equipped with two shunted piezoelectric elements and coupled with an acoustic cavity. This example is analyzed in order to show that the reduced-order model is able to capture the main characteristics of the system dynamical behavior, in particular, in terms of attenuation.

## 2 Finite Element Formulation of the Structural-Acoustic Problem With Piezopatches

We briefly recall in this section the variational formulation of a fluid/structure/piezopatches interaction problem in terms of structural mechanical displacement $u_i$, electric potential $\psi$, and fluid pressure $p$ of the inviscid linear acoustic fluid (for more details, we refer the reader to Refs. [11] and [18]). This coupled formulation is adapted to the general case of an elastic structure equipped with piezoelectric patches (see Fig. 1), as done for structural vibrations in Ref. [19].

Notice that standard indicial notations are used throughout the paper: subscripts $i$, $j$, $k$, and $l$ denote the three-dimensional vectors and tensor components and repeated subscripts imply summation. In addition, a comma indicates a partial derivative and a superposed dot a time derivative.

**2.1 Variational Formulation of the Fluid/Structure/Piezopatches Coupled System.** We consider a piezoelectric structure occupying the domain $\Omega_S$ filled with an inviscid linear acoustic fluid occupying the domain $\Omega_F$. We denote by $\Sigma$ the fluid-structure interface and by $n_i^S$ and $n_i^F$ the unit normals external to $\Omega_S$ and $\Omega_F$, respectively. In Fig. 1, $\Omega_S$ denotes the total structural domain (elastic host structure and piezoelectric patches).

The structure is clamped on a part $\Gamma_u$ and subjected (i) to a given surface force density $F_i^d$ on the complementary part $\Gamma_\sigma$ of its external boundary and (ii) to a pressure field $p$ due to the presence of the fluid on its internal boundary $\Sigma$. The electric boundary conditions are defined by a prescribed electric potential $\psi$, denoted as $\psi^d$, on a part $\Gamma_\psi$ of the boundary of the structure and by a surface density of electric charge $q$, denoted $q^d$, on the remaining part $\Gamma_D$ of the boundary of the structure. Thus, the total structure boundary, denoted $\partial\Omega_S$, is such that $\partial\Omega_S = \Gamma_u \cup \Gamma_\sigma \cup \Sigma = \Gamma_D \cup \Gamma_\psi$ with $\Gamma_u \cap \Gamma_\sigma \cap \Sigma = \Gamma_\psi \cap \Gamma_D = \emptyset$.

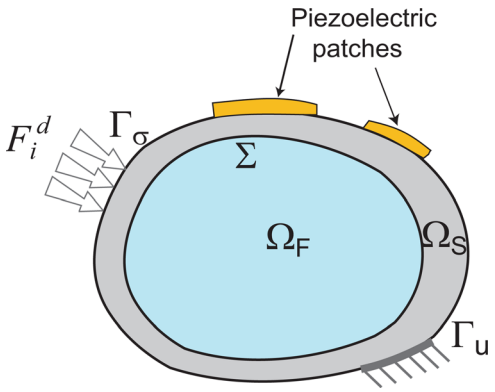


**Fig. 1 Fluid/structure/piezopatches coupled system**

The linearized deformation tensor is $\varepsilon_{ij} = \frac{1}{2}(u_{i,j} + u_{j,i})$, and the stress tensor is denoted by $\sigma_{ij}$. Concerning the electric field variables, $D_i$ is the electric displacement verifying the electric charge equation for a dielectric medium $D_{i,i} = 0$ in $\Omega_S$ and the electric boundary conditions $D_i n_i^S = -q^d$ on $\Gamma_D$. $E_i$ denotes the electric field vector such that $E_i = -\psi_{,i}$.

The linear piezoelectric constitutive equations are

$$\sigma_{ij}(u,\psi) = c_{ijkl}\varepsilon_{kl}(u) - e_{kij}E_k(\psi) \tag{1}$$

$$D_i(u,\psi) = e_{ikl}\varepsilon_{kl}(u) + \varepsilon_{ik}E_k(\psi) \tag{2}$$

where $c_{ijkl}$ denotes the elastic moduli at constant electric field, $e_{kij}$ the piezoelectric constants, and $\varepsilon_{ik}$ the dielectric permittivities at constant strain. Moreover, we denote by $\rho_S$ the mass density of the structure.

Let us consider the special case of an elastic structure (domain $\Omega_E$) equipped with $P$ piezoelectric patches and completely filled with an internal fluid (domain $\Omega_F$). Each piezoelectric patch is covered on its upper and lower surfaces with a very thin layer of conducting material to obtain electrodes. The $p$th patch, $p \in \{1,\cdots,P\}$, occupies a domain $\Omega^{(p)}$ such that $(\Omega_E, \Omega^{(1)},\cdots,\Omega^{(P)})$ is a partition of the all structural domain $\Omega_S$.

A set of hypotheses, which can be applied to a wide spectrum of practical applications, are now formulated:

- The piezoelectric patches are thin, with a constant thickness $h^{(p)}$ for the $p$th patch.
- The thickness of the electrodes is much smaller than $h^{(p)}$ and is thus neglected.
- The piezoelectric patches are polarized in their transverse direction (normal to the electrodes).

Under those assumptions, the electric field vector of components $E_k$ is normal to the electrodes and uniform in the piezoelectric patch (i.e., $E_k = -(V^{(p)}/h^{(p)})n_k$ in $\Omega^{(p)}$ for all $p \in \{1,\cdots,P\}$, where $V^{(p)} = \psi_+^{(p)} - \psi_-^{(p)}$ is the potential difference between the upper and the lower electrode surfaces of the $p$th patch, which is constant over $\Omega^{(p)}$, and $n_k$ is the $k$th component of the normal unit vector to the surface of the electrodes.

By considering successively each of the $P+2$ subdomains $(\Omega_F, \Omega_E, \Omega^{(1)},\cdots,\Omega^{(P)})$, the variational formulation of the fluid/structure/piezopatches coupled system can be written in terms of structural displacement $u_i$, electric potential difference $V^{(p)}$ in each piezoelectric patch, and fluid pressure $p$:

– mechanical equation: $\forall \delta u_i \in \mathcal{C}_u^*$,

$$\int_{\Omega_S} c_{ijkl}\varepsilon_{kl}\delta\varepsilon_{ij}dv + \rho_S \int_{\Omega_S} \frac{\partial^2 u_i}{\partial t^2}\delta u_i dv + \sum_{p=1}^{P} \frac{V^{(p)}}{h^{(p)}} \int_{\Omega^{(p)}} e_{kij} n_k \delta\varepsilon_{ij} dv - \int_{\Sigma} p n_i^F \delta u_i ds = \int_{\Gamma_\sigma} F_i^d \delta u_i ds \tag{3}$$

where $\mathcal{C}_u^*$ is the admissible space of regular functions $u$ defined in $\Omega_S$ and zero on $\Gamma_u$.

– electrical equation: $\forall \delta V^{(p)} \in \mathbb{R}$,

$$\sum_{p=1}^{P} \delta V^{(p)} C^{(p)} V^{(p)} - \sum_{p=1}^{P} \frac{\delta V^{(p)}}{h^{(p)}} \int_{\Omega^{(p)}} e_{ikl}\varepsilon_{kl} n_i dv = \sum_{p=1}^{P} \delta V^{(p)} Q^{(p)} \tag{4}$$

where $C^{(p)} = \varepsilon_{33} S^{(p)}/h^{(p)}$ defines the capacitance of the $p$th piezoelectric patch ($S^{(p)}$ being the surface area of one electrode and $\varepsilon_{33} = \varepsilon_{ik} n_i n_k$ the piezoelectric material permittivity in the direction normal to the electrodes) and $Q^{(p)}$ is the global charge in one of the electrodes (see Ref. [19]).

– acoustical equation: $\forall \delta p \in \mathcal{C}_p$,

$$\frac{1}{\rho_F}\int_{\Omega_F} p_{,i}\delta p_{,i} dv + \frac{1}{\rho_F c_F^2}\int_{\Omega_F} \frac{\partial^2 p}{\partial t^2}\delta p dv + \int_{\Sigma} \frac{\partial^2 u_i}{\partial t^2} n_i^F \delta p ds = 0 \tag{5}$$

where $\mathcal{C}_p$ is the admissible space of regular functions $p$ defined in $\Omega_F$.

Equation (5) corresponds to the variational formulation of the wave equation in the acoustic cavity $p_{,ii} = (1/c_F^2)(\partial^2 p/\partial t^2)$ in $\Omega_F$ together with the boundary condition $p_{,i} n_i^F = -\rho_F(\partial^2 u_i/\partial t^2)\, n_i^F$ on $\Sigma$. This last relation expresses, in terms of $p$ and $u$, the continuity of the normal displacements of the fluid and the structure on $\Sigma$. $c_F$ is the constant speed of sound in the fluid and $\rho_F$ the mass density of the fluid.

Thus, the variational formulation of the fluid/structure/piezopatches coupled problem writes as follows: given $(F^d, \psi^d, q^d)$, find $(u_i \in \mathcal{C}_u^*,\ V^{(p)} \in \mathbb{R},\ p \in \mathcal{C}_p)$ such that Eqs. (3), (4), and (5) are satisfied.

This formulation, with only a couple of electric variables per patch, is well adapted to practical applications, since (i) realistic electrical boundary conditions such that equipotentiality on the electrodes and prescribed global charges naturally appear and (ii) the global charge/voltage variables are intrinsically adapted to include any external electrical circuit into the electromechanical problem and to simulate shunted piezoelectric patches [11,19].

**2.2 Finite Element Discretization of the Fluid/Structure/Piezopatches Coupled System.** Let us introduce $\mathbf{U}$ (of length $N_s$) and $\mathbf{P}$ (of length $N_f$), corresponding to the vectors of nodal values of $u_i$ and $p$, respectively, and $\mathbf{Q} = (Q^{(1)}Q^{(2)}\cdots Q^{(P)})^T$ and $\mathbf{V} = (V^{(1)}V^{(2)}\cdots V^{(P)})^T$ the column vectors of electric charges and potential differences. Thus, the variational Eqs. (3), (4), and (5) for the fluid/structure/piezoelectric patches coupled problem can be written, in discretized form, as the following unsymmetric matrix system:

$$\begin{bmatrix} \mathbf{M}_u & \mathbf{0} & \mathbf{0} \\ \mathbf{0} & \mathbf{0} & \mathbf{0} \\ \mathbf{C}_{up}^T & \mathbf{0} & \mathbf{M}_p \end{bmatrix} \begin{bmatrix} \ddot{\mathbf{U}} \\ \ddot{\mathbf{V}} \\ \ddot{\mathbf{P}} \end{bmatrix} + \begin{bmatrix} \mathbf{K}_u & \mathbf{C}_{uV} & -\mathbf{C}_{up} \\ -\mathbf{C}_{uV}^T & \mathbf{K}_V & \mathbf{0} \\ \mathbf{0} & \mathbf{0} & \mathbf{K}_p \end{bmatrix} \begin{bmatrix} \mathbf{U} \\ \mathbf{V} \\ \mathbf{P} \end{bmatrix} = \begin{bmatrix} \mathbf{F} \\ \mathbf{Q} \\ \mathbf{0} \end{bmatrix} \tag{6}$$

where $\mathbf{M}_u$ and $\mathbf{K}_u$ are the mass and stiffness matrices of the structure; $\mathbf{C}_{uV}$ is the electric mechanical coupled stiffness matrix; $\mathbf{K}_V = \mathrm{diag}\left(C^{(1)}C^{(2)}\cdots C^{(P)}\right)$ is a diagonal matrix filled with the $P$ capacitances of the piezoelectric patches; $\mathbf{M}_p$ and $\mathbf{K}_p$ are the mass and stiffness matrices of the fluid; $\mathbf{C}_{up}$ is the fluid-structure coupled matrix; and $\mathbf{F}$ is the applied mechanical force vector. These submatrices correspond to the various linear and bilinear forms involved in Eqs. (3), (4), and (5).

Note that Eq. (6) must be completed by appropriate initial conditions and could be symmetrized as done in Ref. [14].

**2.3 Structural-Acoustic Problem With Piezopatches Connected to RL Series Shunt Circuit.** The above discretized formulation defined by Eq. (6) can be used for a wide range of applications of mechanical structures with piezoelectric patches coupled with acoustic domain. It is particularly adapted to the case where the piezoelectric patches are shunted (i.e., connected to a passive electrical network [8]). In this case, neither $\mathbf{V}$ nor $\mathbf{Q}$ are prescribed by the electrical network, but the latter imposes a relation between them. In the case of a resonant shunt connected to the $p$th patch and composed of a resistance $R^{(p)}$ and an inductance $L^{(p)}$ in series (Fig. 2), we have the following additional constraint between electrical potential differences $\mathbf{V}$ and the electric charges $\mathbf{Q}$:

$$\mathbf{L}\ddot{\mathbf{Q}} + \mathbf{R}\dot{\mathbf{Q}} + \mathbf{V} = \mathbf{0} \tag{7}$$

where $\mathbf{R} = \mathrm{diag}\left(R^{(1)}R^{(2)}\cdots R^{(P)}\right)$ and $\mathbf{L} = \mathrm{diag}\left(L^{(1)}L^{(2)}\cdots L^{(P)}\right)$ are diagonal matrices filled with the $P$ resistances and inductances of the shunt circuits.

Due to the direct piezoelectric effect, the piezoelectric patch converts a fraction of the mechanical energy of the vibrating structure into electrical energy, which can be dissipated through the resistive components of the $RL$ circuit. It is well known that the damping effect due to this circuit is maximal when the resonance circular frequency $1/\sqrt{LC}$ of the shunt circuit is tuned in the circular frequency of the structural-acoustic eigenmode to be controlled. The resistance $R$ and the inductance $L$ can be adjusted and properly chosen to maximize the damping effect of a particular mode (see, for example, Refs. [8], [20], and [21]). The optimal resistance and inductance for the $i$th mode and for a series resonant shunt are given by

$$R^{\mathrm{opt}} = \frac{\sqrt{2k_{\mathrm{eff},i}^2}}{C\omega_i(1+k_{\mathrm{eff},i}^2)} \tag{8a}$$

$$L^{\mathrm{opt}} = \frac{1}{C\omega_i^2(1+k_{\mathrm{eff},i}^2)} \tag{8b}$$

where $\omega_i$ is the short-circuit natural frequency and $k_{\mathrm{eff},i}$ is the effective electromechanical coupling coefficient given by

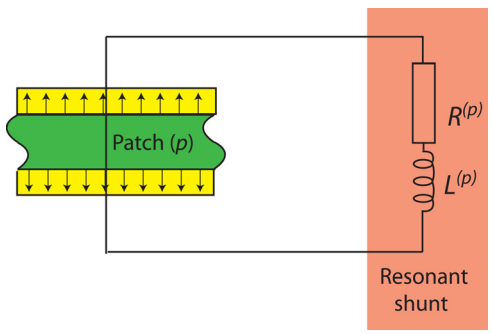


**Fig. 2 Piezoelectric patch connected to RL-shunt circuit**

$$k_{\text{eff},i} = \sqrt{\frac{\hat{\omega}_i^2 - \omega_i^2}{\omega_i^2}} \tag{9}$$

$\hat{\omega}_i$ being the open-circuit $i$th natural frequency.

Using the second row of Eq. (6), the degrees-of-freedom associated with the electrical potential difference $\mathbf{V}$ can be expressed in terms of structural displacements $\mathbf{U}$ and electric charge $\mathbf{Q}$ as

$$\mathbf{V} = \mathbf{K}_V^{-1}\mathbf{C}_{uV}^T\mathbf{U} + \mathbf{K}_V^{-1}\mathbf{Q} \tag{10}$$

Thus, after substituting this expression of $\mathbf{V}$ into Eq. (7) and using Eq. (6), we get the following electromechanical-acoustic matrix system:

$$\begin{bmatrix} \mathbf{M}_u & \mathbf{0} & \mathbf{0} \\ \mathbf{0} & \mathbf{L} & \mathbf{0} \\ \mathbf{C}_{up}^T & \mathbf{0} & \mathbf{M}_p \end{bmatrix} \begin{bmatrix} \ddot{\mathbf{U}} \\ \ddot{\mathbf{Q}} \\ \ddot{\mathbf{P}} \end{bmatrix} + \begin{bmatrix} \mathbf{0} & \mathbf{0} & \mathbf{0} \\ \mathbf{0} & \mathbf{R} & \mathbf{0} \\ \mathbf{0} & \mathbf{0} & \mathbf{0} \end{bmatrix} \begin{bmatrix} \dot{\mathbf{U}} \\ \dot{\mathbf{Q}} \\ \dot{\mathbf{P}} \end{bmatrix} + \begin{bmatrix} \mathbf{K}_u + \mathbf{C}_{uV}\mathbf{K}_V^{-1}\mathbf{C}_{uV}^T & \mathbf{C}_{uV}\mathbf{K}_V^{-1} & -\mathbf{C}_{up} \\ \mathbf{K}_V^{-1}\mathbf{C}_{uV}^T & \mathbf{K}_V^{-1} & \mathbf{0} \\ \mathbf{0} & \mathbf{0} & \mathbf{K}_p \end{bmatrix} \begin{bmatrix} \mathbf{U} \\ \mathbf{Q} \\ \mathbf{P} \end{bmatrix} = \begin{bmatrix} \mathbf{F} \\ \mathbf{0} \\ \mathbf{0} \end{bmatrix} \tag{11}$$

This ($\mathbf{U}$, $\mathbf{Q}$, $\mathbf{P}$) formulation is also well-suited for switched shunt techniques [11]. Let us remark that no structural damping has been introduced at this stage but will be considered under the standard form of a modal damping in the reduced-order model presented in Sec. 3.

## 3 Reduced-Order Model

In this section, we introduce a reduced-order formulation of the variational Eqs. (3), (4), and (5) by a Ritz–Galerkin projection on two bases spanning the admissible spaces $\mathcal{C}_u^*$ and $\mathcal{C}_p$. Note that the chosen reduction concerns only the mechanical variables $\mathbf{U}$ and $\mathbf{P}$. The electrical unknown field $\mathbf{Q}$ is not concerned by the reduction because the dimension of this vector corresponds to the number of piezopatches and therefore is very small compared to the mechanical finite element degrees-of-freedom (i.e., pressure in the fluid and displacement in the host structure and the piezopatches). For $\mathcal{C}_u^*$, we use the in vacuo structural modes in short-circuit configuration, which can be computed using a standard elastic formulation. Concerning $\mathcal{C}_p$, the basis is formed by the eigenmodes of the Helmholtz equation $p_{,ii} = (\omega^2/c_F^2)p$, in which $\omega$ is the circular frequency, with the boundary condition $(\partial p/\partial n_F) = 0$ corresponding to the fixed rigid cavity.

**3.1 Remark on the Physical Static Acoustic Problem.** The physical acoustic modes in a rigid fixed cavity are such that their mean value over the acoustic domain $\Omega_F$ is zero (i.e., $\int_{\Omega_F} p dv = 0$). In effect, for harmonic vibrations, the variational Eq. (5), restricted to a rigid fixed cavity (i.e., $u_i n_i^F = 0$ on $\Sigma$) writes, for $p \in \mathcal{C}_p$ and $\forall \delta p \in \mathcal{C}_p$,

$$\int_{\Omega_F} p_{,i}\delta p_{,i} dv - \frac{\omega^2}{c_F^2}\int_{\Omega_F} p\delta p dv = 0 \tag{12}$$

This Eq. (12) shows that $\omega = 0$ and $p = C_0$ ($C_0$ being a constant over $\Omega_F$) is an eigensolution. The orthogonality between this eigenmode ($\omega = 0$) and any other eigenmode ($\omega \neq 0$) writes $\int_{\Omega_F} pC_0 dv = 0$ and then $\int_{\Omega_F} p dv = 0$. It is important to note that the eigensolution ($\omega = 0$, $p = C_0$) is not physical, because it does not correspond to any interpretation of rigid body motion—as it is the case for free-free structural vibration—the wall being rigid and fixed. Nevertheless, in the variational formulation in Eq. (5), the admissible space $\mathcal{C}_p$ must include this particular solution in order to have a complete basis. Alternatively, the formulation in Eqs. (3), (4), and (5) can be regularized for zero frequency situation (i.e., valid for a static problem) by adding the following constraint: $\rho_F c_F^2 \int_\Sigma u_i n_i ds + \int_{\Omega_F} p dv = 0$ (see Ref. [15] for details). When doing this, on one hand the static pressure is defined precisely by $p^s = -(\rho_F c_F^2/|\Omega_F|)\int_\Sigma u_i n_i ds$ and, on the other hand, the reduced-order formulation will be carried only by projection on the physical acoustic modes. This alternative formulation is not used in this paper but is the subject of further investigations.

**3.2 Eigenmodes of the Structure In Vacuo With Short-Circuited Patches.** In a first step, the first $M_s$ eigenmodes of the structure in vacuo with all patches short-circuited are obtained from the following equation:

$$\left(\mathbf{K}_u - \omega_{si}^2\mathbf{M}_u\right)\mathbf{\Phi}_{si} = \mathbf{0} \quad \text{for } i \in \{1, \cdots, M_s\} \tag{13}$$

where $(\omega_{si}, \mathbf{\Phi}_{si})$ are the natural frequency and eigenvector for the $i$th structural mode. These modes verify the following orthogonality properties:

$$\mathbf{\Phi}_{si}^T\mathbf{M}_u\mathbf{\Phi}_{sj} = \delta_{ij} \quad \text{and} \quad \mathbf{\Phi}_{si}^T\mathbf{K}_u\mathbf{\Phi}_{sj} = \omega_{si}^2\delta_{ij} \tag{14}$$

where $\delta_{ij}$ is the Kronecker symbol and $\mathbf{\Phi}_{si}$ have been normalized with respect to the structure mass matrix. Note that the structure is fixed on $\Gamma_u$, which eliminates any rigid body motion.

**3.3 Eigenmodes Associated With the Rigid Acoustic Cavity.** In a second step, the first $M_f$ eigenmodes of the acoustic cavity with rigid boundary conditions are obtained from the following equation, corresponding to the finite element discretization of Eq. (12):

$$\left(\mathbf{K}_p - \omega_{fi}^2\mathbf{M}_p\right)\mathbf{\Phi}_{fi} = \mathbf{0} \quad \text{for } i \in \{1, \cdots, M_f\} \tag{15}$$

where $(\omega_{fi}, \mathbf{\Phi}_{fi})$ are the natural frequency and eigenvector for the $i$th acoustic mode. Referring to the first paragraph of this section, we have $\omega_{f1} = 0$ and $\mathbf{\Phi}_{f1} = C_0\mathbf{1}$, where $\mathbf{1}$ is an identity vector. These modes verify the following orthogonality properties:

$$\mathbf{\Phi}_{fi}^T\mathbf{M}_p\mathbf{\Phi}_{fj} = \delta_{ij} \quad \text{and} \quad \mathbf{\Phi}_{fi}^T\mathbf{K}_p\mathbf{\Phi}_{sj} = \omega_{fi}^2\delta_{ij} \tag{16}$$

where $\mathbf{\Phi}_{fi}$ have been normalized with respect to the fluid mass matrix.

The orthogonality relationship in Eq. (16) with respect to the constant vector writes

$$C_0\mathbf{1}^T\mathbf{M}_p\mathbf{\Phi}_{fj} = 0 \quad \text{for } j \in \{2, \cdots, M_f\} \tag{17}$$

This equation corresponds to the finite element discretized of the zero mean value of the physical pressure $p$ over the acoustic domain $\Omega_F$. This is taken into account inside the eigenvalue algorithm of the finite element code (for instance, if an iteration method is used).

**3.4 Reduced-Order System in Terms of ($\mathbf{q}_s$, $\mathbf{Q}$, $\mathbf{q}_f$).** By introducing the matrices $\mathbf{\Phi}_s = [\mathbf{\Phi}_{s1} \cdots \mathbf{\Phi}_{sM_s}]$ of size $N_s \times M_s$ and $\mathbf{\Phi}_f = [\mathbf{\Phi}_{f1} \cdots \mathbf{\Phi}_{fM_f}]$ of size $N_f \times M_f$ corresponding to the two bases previously defined, $\mathbf{U}$ and $\mathbf{P}$ are sought as

$$\mathbf{U} = \mathbf{\Phi}_s\mathbf{q}_s(t) \quad \text{and} \quad \mathbf{P} = \mathbf{\Phi}_f\mathbf{q}_f(t) \tag{18}$$

where the vectors $\mathbf{q}_s = [q_{s1} \cdots q_{sM_s}]^T$ and $\mathbf{q}_f = [q_{f1} \cdots q_{fM_f}]^T$ are the unknown coordinates.

By applying the Ritz–Galerkin projection method, which consists of substituting relations in Eq. (18) into Eq. (11) and

premultiplying the first row by $\mathbf{\Phi}_s^T$ and the third one by $\mathbf{\Phi}_f^T$, we obtain the reduced matrix system,

$$\begin{bmatrix} \mathbf{\Phi}_s^T\mathbf{M}_u\mathbf{\Phi}_s & \mathbf{0} & \mathbf{0} \\ \mathbf{0} & \mathbf{L} & \mathbf{0} \\ \mathbf{\Phi}_f^T\mathbf{C}_{up}^T\mathbf{\Phi}_s & \mathbf{0} & \mathbf{\Phi}_f^T\mathbf{M}_p\mathbf{\Phi}_f \end{bmatrix} \begin{bmatrix} \ddot{\mathbf{q}}_s \\ \ddot{\mathbf{Q}} \\ \ddot{\mathbf{q}}_f \end{bmatrix} + \begin{bmatrix} \mathbf{0} & \mathbf{0} & \mathbf{0} \\ \mathbf{0} & \mathbf{R} & \mathbf{0} \\ \mathbf{0} & \mathbf{0} & \mathbf{0} \end{bmatrix} \begin{bmatrix} \dot{\mathbf{q}}_s \\ \dot{\mathbf{Q}} \\ \dot{\mathbf{q}}_f \end{bmatrix}$$
$$+ \begin{bmatrix} \mathbf{\Phi}_s^T\left(\mathbf{K}_u + \mathbf{C}_{uV}\mathbf{K}_V^{-1}\mathbf{C}_{uV}^T\right)\mathbf{\Phi}_s & \mathbf{\Phi}_s^T\mathbf{C}_{uV}\mathbf{K}_V^{-1} & -\mathbf{\Phi}_s^T\mathbf{C}_{up}\mathbf{\Phi}_f \\ \mathbf{K}_V^{-1}\mathbf{C}_{uV}^T\mathbf{\Phi}_s & \mathbf{K}_V^{-1} & \mathbf{0} \\ \mathbf{0} & \mathbf{0} & \mathbf{\Phi}_f^T\mathbf{K}_p\mathbf{\Phi}_f \end{bmatrix}$$
$$\times \begin{bmatrix} \mathbf{q}_s \\ \mathbf{Q} \\ \mathbf{q}_f \end{bmatrix} = \begin{bmatrix} \mathbf{\Phi}_s^T\mathbf{F} \\ \mathbf{0} \\ \mathbf{0} \end{bmatrix}$$

This matrix equation represents the reduced-order model of the structural-acoustic problem with piezoelectric shunt-damping treatments. If only few modes are kept for the projection, the size of this reduced-order model ($M_s \times P \times M_f$) is much smaller than the initial one ($N_s \times P \times N_f$).

Equation (19) can be also written in the following form of coupled differential equations:

– $M_s$ mechanical equations

$$\ddot{q}_{si} + 2\xi_i\omega_{si}\dot{q}_{si} + \omega_{si}^2 q_{si} + \sum_{p=1}^{P}\sum_{k=1}^{M_s}\frac{\gamma_i^{(p)}\gamma_k^{(p)}}{C^{(p)}}q_{si} + \sum_{p=1}^{P}\frac{\gamma_i^{(p)}}{C^{(p)}}Q^{(p)} - \sum_{j=1}^{M_f}\beta_{ij}q_{fj} = F_i \tag{20}$$

– $P$ electrical equations

$$L^{(p)}\ddot{Q}^{(p)} + R^{(p)}\dot{Q}^{(p)} + \frac{Q^{(p)}}{C^{(p)}} + \sum_{i=1}^{N_s}\frac{\gamma_i}{C^{(p)}}q_{si} = 0 \tag{21}$$

– $M_f$ acoustical equations

$$\ddot{q}_{fi} + \omega_{fi}^2 q_{fi} + \sum_{j=1}^{M_s}\beta_{ij}q_{sj} = 0 \tag{22}$$

where $F_i(t) = \mathbf{\Phi}_{si}^T\mathbf{F}$ is the mechanical excitation of the i*th* mode, $\beta_{ij} = \mathbf{\Phi}_{si}^T\mathbf{C}_{up}\mathbf{\Phi}_{fj}$ are the fluid structure coupling coefficients, and $\gamma_i = \mathbf{\Phi}_{si}^T\mathbf{C}_{uV}$ the electromechanical coupling factors.

Note that the modal damping coefficients $\xi_i$ have been added in Eq. (20) but not in Eq. (19), in order to take into account the structural damping, which can be measured experimentally. This is mandatory in order to quantify the attenuation due to the shunt at the resonance (of course, without damping, the amplitude of the response at the resonance is theoretically infinite).

The formulation in terms of physical variables (**U**, **Q**, **P**) has been replaced by the reduced formulation in terms of hybrid coordinates ($\mathbf{q}_s$, **Q**, $\mathbf{q}_f$). Its major interest, and especially the choice of the short-circuit eigenmodes as the expansion basis, is that the above computations of the parameters necessitate only a modal analysis of an elastic problem. This operation can thus be done using any standard finite element code. In Sec. 4, as our purpose is to verify the reliability and the precision of the reduced model, we carried out numerical experimentation. The problem of mode truncation is analyzed through several computations obtained by varying the number of structural and acoustic modes in relation with the frequency band of interest. The acceleration of convergence by using appropriate static corrections has not been included in the following example but will be the subject of further investigations.

## 4 Numerical Example

We consider a 3D acoustic cavity completely filled with air (density $\rho_F = 1.2$ kg/m$^3$; speed of sound $c_F = 340$ m/s). The cavity walls are rigid except the top one, which is a flexible aluminum plate of thickness 1 mm clamped at its four edges. This particular configuration has been chosen because it gives preliminary results concerning noise and vibration in a usual shape of a demonstrator (small size mock-up of an automobile). More precisely, the chosen system can be checked experimentally without being too costly, because the geometry is constituted by an assembly of simple subsystems, namely, an elastic plate and rigid rectangular walls. It should be noted that similar but more complex configurations have been used for structural-acoustic analyses in various references (see, for example, Refs. [17] and [22]). The density of the plate is 2700 kg/ m$^3$, the Young modulus 72 GPa, and the Poisson ratio 0.34. On the top surface of the plate, two identical piezoelectric patches of thickness 0.5 mm are bonded. For the mechanical characteristics of the piezoelectric material PIC151, the reader can be referred to Ref. [19]. The geometrical data and the finite element mesh are presented in Fig. 3.

Concerning the finite element discretization, we have used for the structural part 200 four-node plate elements based on Mindlin theory with five degrees-of-freedom per node (i.e., $N_s = 1155$). The portions of the plate covered by the piezoelectric patches have been modeled according to the first-order shear deformation laminated theory [23]. As discussed in Secs. 1–3, only one electrical degree of freedom is used to represent the electrical charge $Q$ in each patch. The acoustic cavity is discretized using 2600 hexahedric elements with one degree-of-freedom per node, corresponding to the acoustic pressure (i.e., $N_f = 3234$). Note that the structural and acoustic meshes are compatible at the interface. The frequency range considered in this example is 0–500 Hz.

**4.1 Modal Analysis of the Acoustic/Structure/Piezopatches Coupled Problem.** Table 1 presents the eigenfrequencies in three cases: (i) the 3D rigid acoustic cavity; (ii) the clamped plate with the two patches short-circuited; and (iii) the plate/acoustic-cavity coupled system in the short-circuit case. All coupled frequencies, except the sixth, are associated with the vibration modes of the structure lower than 450 Hz. The sixth frequency of the coupled problem corresponds to the first acoustic mode in rigid cavity. This can be confirmed by comparing the mode shapes in case (iii) with those obtained in cases (i) or (ii), which are not shown here for sake of brevity. Moreover, let us remark that the natural frequencies of the coupled modes (where the structural deformation is predominant) are lower than those for the structure in vacuo, except for the first mode, which is also the most affected by the presence of the fluid cavity. For illustration purpose, Fig. 4 shows the deformed plate and the pressure field for the first ten vibration modes in the coupled case. Moreover, direct frequency response functions without damping and with short-circuited patches are calculated using Eq. (6) written in the frequency domain. The obtained curves, presented in Fig. 5, show the resonances of the coupled system, which are in perfect correlation with the eigenfrequencies of the coupled problem (see the third column of Table 1). The mechanical transverse displacement in the plate is evaluated at the point of coordinates ($x = 0.14$ m, $y = 0.06$ m, $z = 0.3$ m) and the sound pressure level in the acoustic cavity at the point of coordinates ($x = 0.15$ m, $y = 0.09$ m, $z = 0.1$ m). It should be noted that

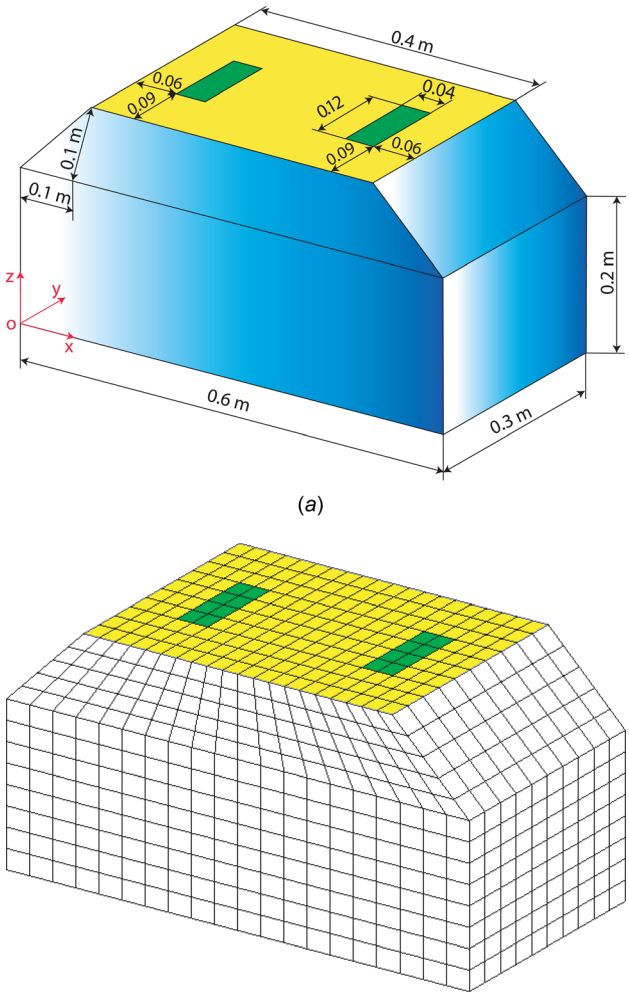


(*a*)

(*b*)

**Fig. 3 Geometrical data and finite element mesh of the acoustic/structure/patches system: (*a*) geometrical data and (*b*) finite element mesh**

**Table 1 Computed frequencies (in Hz) of the structural-acoustic coupled system**

| Fluid in a rigid cavity | Structure in vacuo | Coupled modes | Type[a] |
|---|---|---|---|
| 297.94 | 77.93 | 85.40 | S |
| 561.56 | 123.64 | 122.53 | S |
| 569.00 | 194.29 | 192.79 | S |
| 614.82 | 212.29 | 211.94 | S |
| 642.29 | 237.12 | 236.14 | S |
| 681.94 | 316.11 | 298.31 | F |
| 799.44 | 346.32 | 315.59 | S |
| 837.71 | 383.89 | 346.24 | S |
| 875.22 | 434.73 | 382.23 | S |
| 881.62 | 451.03 | 433.61 | S |

[a]S for structure predominant modal shape and F for fluid predominant modal shape.

the responses are not infinite (at it should be theoretically, due to the absence of damping) because the calculations are made by a frequency sweeping.

**4.2 Dynamic Response of the Acoustic/Structure/Piezopatches Coupled Problem.** In this part, shunt systems connected with two piezoelectric patches (see Fig. 6) are used in

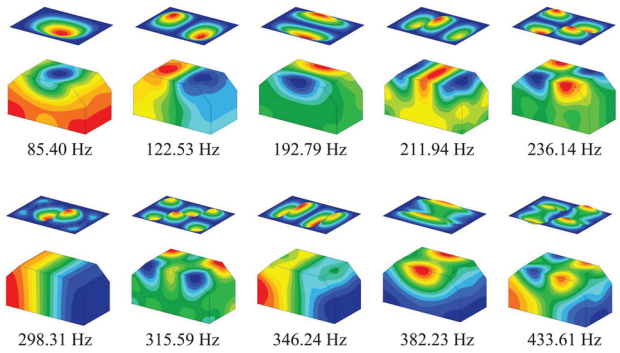


**Fig. 4 First ten fluid-structure coupled modes: fluid pressure level in the cavity and plate total displacement**

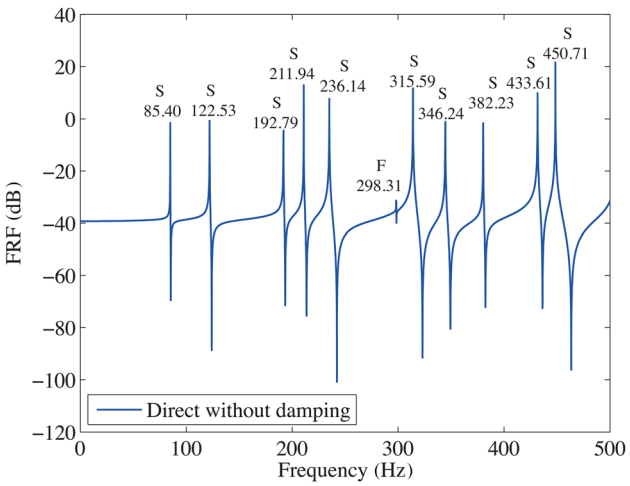


(*a*)

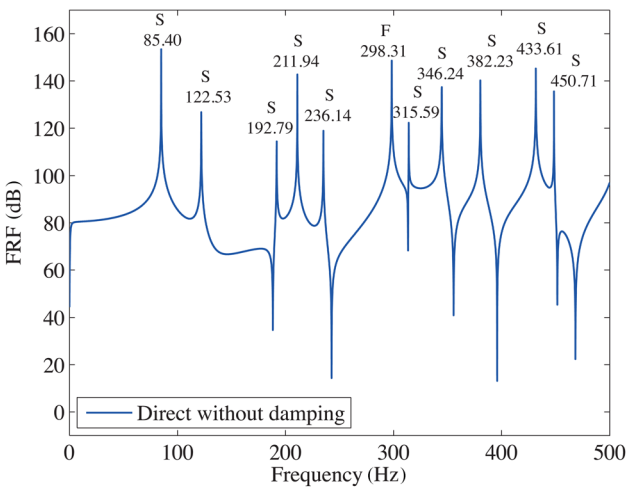


(*b*)

**Fig. 5 Displacement and pressure responses of the full-order model without damping: (*a*) mechanical transverse displacement in the plate and (*b*) sound pressure level in the acoustic cavity**

order to get a multimodal damping of the coupled system. The chosen objective is to attenuate the second and fourth modes of the plate. For this purpose, the patches are tuned independently and simultaneously using Eqs. (8*a*) and (8*b*). The optimal values of the shunt electrical parameters are then, respectively, $R_1 = 632\ \Omega$ and $L_1 = 9.5\,\text{H}$ for the second mode and $R_2 = 735\ \Omega$ and $L_2 = 3.2\,\text{H}$ for the fourth mode. The two modes being well separated within the frequency band (shift around 90 Hz, as it can be

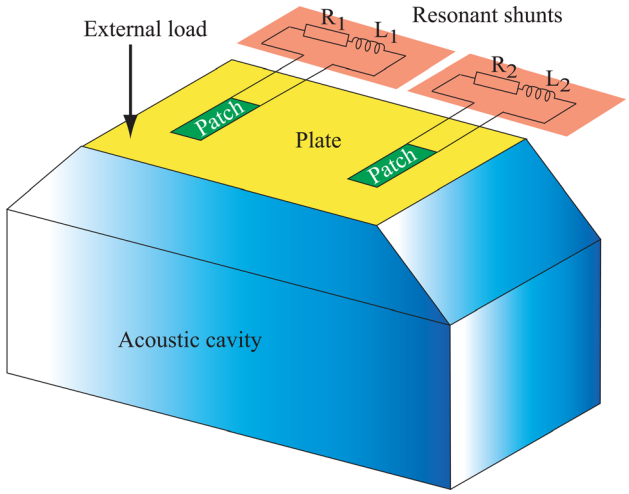


**Fig. 6 Structural-acoustic coupled problem with two piezoelectric patches connected to RL-shunt circuits**

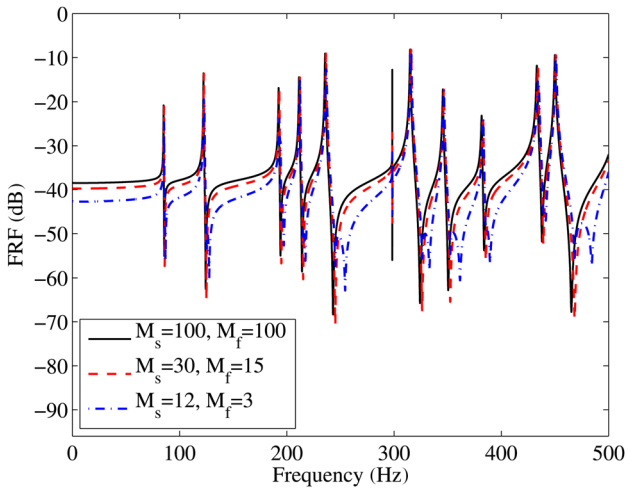


(*a*)

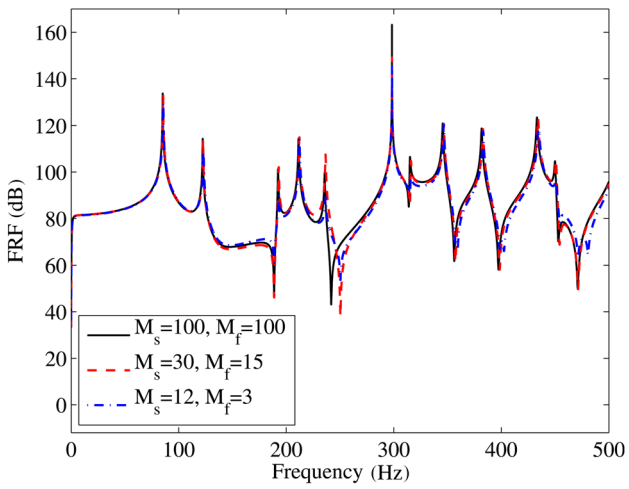


(*b*)

**Fig. 7 Influence of the structural and acoustic mode truncation on the response of the reduced-order model with structural damping: (*a*) mechanical transverse displacement in the plate and (*b*) sound pressure level in the acoustic cavity**

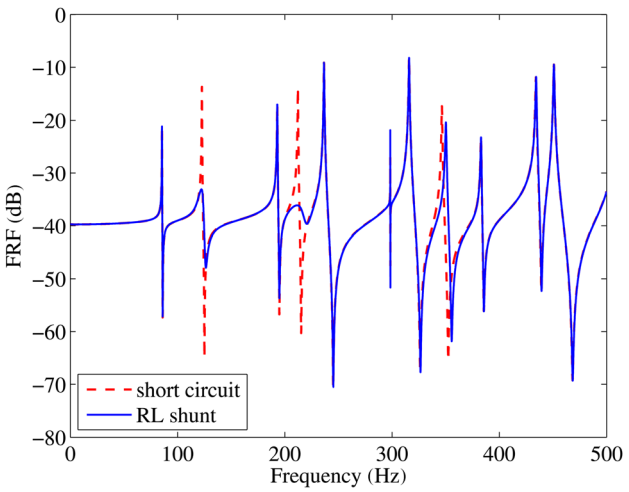


(*a*)

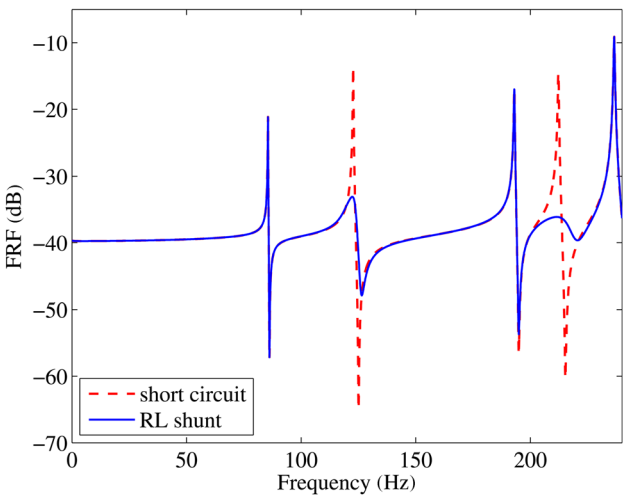


(*b*)

**Fig. 8 Frequency response function: transverse displacement amplitude in dB at the excitation point within the frequency band 0–500 Hz (*a*) and 0–250 Hz (*b*)**

seen in Table 1 or Figs. 8 and 9), we consider that there is only a weak interference between them. Each patch is then connected to one shunt for the attenuation of one mode. The plate is excited by a mechanical force of intensity 1 N located at ($x = 0.14$ m, $y = 0.06$ m, $z = 0.3$ m). A constant structural damping ratio has been used in the simulation ($\xi_i = 0.5\%$). Note that no damping has been introduced in the acoustic fluid due to the limited frequency range of interest [24].

The system vibratory response is obtained with the modal reduction approach defined by Eq. (19). In order to evaluate the number of structural and acoustic modes to keep in the modal projection, various simulations have been performed. Three cases are then analyzed: (i) $M_s = 100$ and $M_f = 100$, which corresponds to a frequency range much beyond 0–500 Hz; (ii) $M_s = 12$ (515 Hz) and $M_f = 3$ (562 Hz), which corresponds approximately to the frequency of interest; and (iii) $M_s = 30$ (1297 Hz) and $M_f = 15$ (1072 Hz), which is slightly higher than the double of the frequency of interest. We recall that, in the three cases, the constant mode at zero frequency for the fluid corresponds to the first one. We consider that $M_s = 30$ and $M_f = 15$ is satisfying in comparison with the case $M_s = 100$ and $M_f = 100$ (see Fig. 7). The discrepancies observed at the antiresonances do not play an important role here because we are only interested in the attenuation at the resonances and do not perform an active control of the

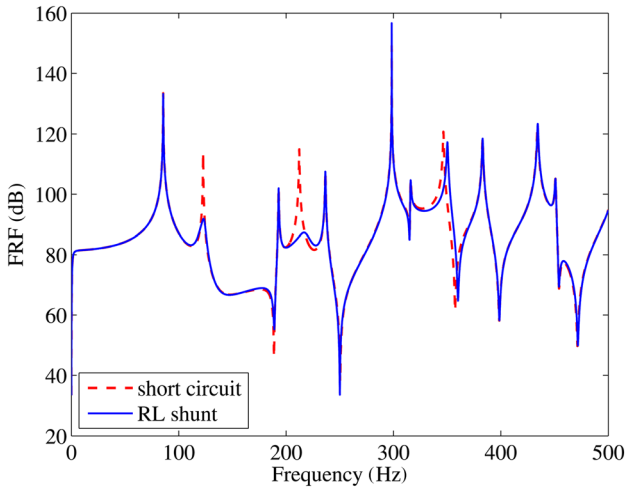


(*a*)

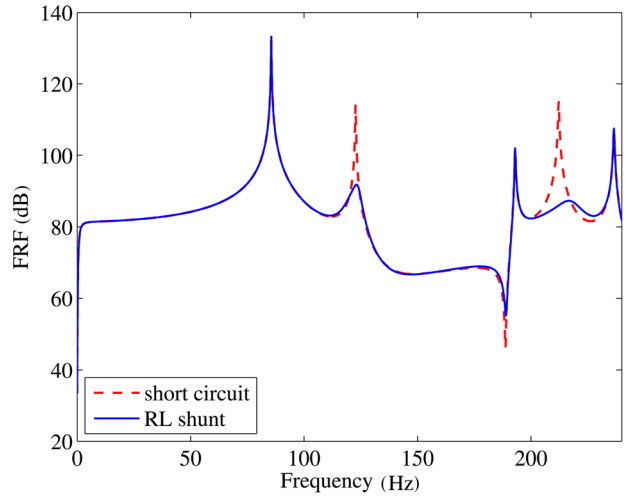


(*b*)

**Fig. 9 Frequency response function: pressure level in dB at ($x = 50.15$ m, $y = 50.09$ m, and $z = 50.1$ m) within the frequency b and 0–500 Hz (*a*) and 0–250 Hz (*b*)**

system. A deep study of truncation effects, acceleration of convergence, and error estimation, using, for example, various static corrections, is presently under investigation but outside the scope of this paper.

Figures 8 and 9 present the frequency response functions of the reduced-order model with and without shunt (at the same structural and fluid points as in the full-order model of Sec. 4.1). Referring to the preceding analysis, these results are obtained using 30 structural modes ($M_s = 30$) and 15 acoustic modes ($M_f = 15$). These figures show that the modal resonant magnitude for each considered mode has been significantly reduced (around 20 dB). In fact, the strain energy present in the piezoelectric material is converted into electrical energy and then efficiently dissipated into heat by the RL-shunt devices.

## 5 Conclusion

In this work, an original reduced-order formulation of structural-acoustic problems with piezoelectric patches is presented. This formulation, involving only a couple of electric variables by patch, allows taking into account naturally realistic electric boundary conditions. The proposed methodology requires the computation of the eigenmodes of the structure with short-circuited piezoelectric patches and the rigid acoustic cavity. It is shown that the projection of the full-order coupled finite element model on the subspace spanned by the uncoupled bases leads to a reduced-order model in which the main parameters are the classical fluid-structure and electromechanical modal coupling factors. Despite its reduced size, this model is proven to be very efficient for simulations of steady-state analyses of structural-acoustic coupled systems with shunt damping. Further investigations will concern symmetrization, acceleration of convergence, as well as introduction of additional passive dissipation in the fluid and at the interface.

## References


[1] Balachandran, B., Sampath, A., and Park, J., 1996, "Active Control of Interior Noise in a Three-Dimensional Enclosure," Smart Mater. Struct., **5**(1), pp. 89–97.

[2] Ahmadian, M., Jeric, K., and Inman, D., 2001, "An Experimental Evaluation of Smart Damping Materials for Reducing Structural Noise and Vibrations," ASME J. Vibr. Acoust., **123**(4), pp. 533–536.

[3] Kim, J., Ko, B., Lee, J. K., and Cheong, C., 1999, "Finite Element Modelling of a Piezoelectric Smart Structure for the Cabin Noise Problem," Smart Mater. Struct., **8**(3), pp. 380–389.

[4] Lefevre, J., and Gabbert, U., 2005, "Finite Element Modeling of Vibro-Acoustic Systems for Active Noise Reduction," Tech. Mech., **25**(3-4), pp. 241–247.

[5] Ro, J., and Baz, A., 1999, "Control of Sound Radiation From a Plate Into an Acoustic Cavity Using Active Constrained Layer Damping," Smart Mater. Struct., **8**(3), pp. 292–300.

[6] Kaljevic, I., and Saravanos, D., 1997, "Steady State Response of Acoustic Cavities Bounded by Piezoelectric Composite Shell Structures," J. Sound Vibr., **204**(3), pp. 459–476.

[7] Gopinathan, S., Varadan, V., and Varadan, V., 2000, "Finite Element/Boundary Element Simulation of Interior Noise Control Using Active-Passive Control Technique," Proc. SPIE, **3984**, pp. 22–32.

[8] Hagood, N. W., and Flotow, A. V., 1991, "Damping of Structural Vibrations With Piezoelectric Materials and Passive Electrical Networks," J. Sound Vibr., **146**(2), pp. 243–268.

[9] Lesieutre, G. A., 2008, "Vibration Damping and Control Using Shunted Piezoelectric Materials," Shock Vibr. Dig., **30**(3), pp. 187–195.

[10] Guyomar, D., Richard, T., and Richard, C., 2008, "Sound Wave Transmission Reduction Through a Plate Using a Piezoelectric Synchronized Switch Damping Technique," J. Intell. Mater. Syst. Struct., **19**(7), pp. 791–803.

[11] Larbi, W., Deü, J.-F., Ciminello, M., and Ohayon, R., 2010, "Structural-Acoustic Vibration Reduction Using Switched Shunt Piezoelectric Patches: A Finite Element Analysis," ASME J. Vibr. Acoust., **132**(5), p. 051006.

[12] Craggs, A., and Stead, G., 1976, "Sound Transmission Between Enclosures—A Study Using Plate and Acoustic Finite Elements," Acustica, **35**(2), pp. 89–98.

[13] Daniel, W., 1980, "Performance of Reduction Methods for Fluid-Structure and Acoustic Eigenvalue Problems," Int. J. Numer. Methods Eng., **15**(11), pp. 1585–1594.

[14] Morand, H., and Ohayon, R., 1995, *Fluid-Structure Interaction*, Wiley, New York.

[15] Ohayon, R., 2004, "Reduced Models for Fluid-Structure Interaction Problems," Int. J. Numer. Methods Eng., **60**(1), pp. 139–152.

[16] Al-Bassyiouni, M., and Balachandran, B., 2005, "Sound Transmission Through a Flexible Panel Into an Enclosure: Structural-Acoustics Model," J. Sound Vibr., **284**(1-2), pp. 467–486.

[17] Puri, R. S., and Morrey, D., 2011, "A Krylov–Arnoldi Reduced Order Modelling Framework for Efficient, Fully Coupled, Structural–Acoustic Optimization," Struct. Multidisc. Optim., **43**(4), pp. 495–517.

[18] Deü, J.-F., Larbi, W., and Ohayon, R., 2008, "Piezoelectric Structural Acoustic Problems: Symmetric Variational Formulations and Finite Element Results," Comput. Methods Appl. Mech. Eng., **197**(19-20), pp. 1715–1724.

[19] Thomas, O., Deü, J.-F., and Ducarne, J., 2009, "Vibrations of an Elastic Structure With Shunted Piezoelectric Patches: Efficient Finite Element Formulation and Electromechanical Coupling Coefficients," Int. J. Numer. Methods Eng., **80**(2), pp. 235–268.

[20] Corr, L., and Clark, W., 2002, "Comparison of Low-Frequency Piezoelectric Switching Shunt Techniques for Structural Damping," Smart Mater. Struct., **11**(3), pp. 370–376.

[21] Thomas, O., Ducarne, J., and Deü, J.-F., 2012, "Performance of Piezoelectric Shunts for Vibration Reduction," Smart Mater. Struct., **21**(1), p. 015008.

[22] Rumpler, R., Legay, A., and Deü, J.-F., 2011, "Performance of a Restrained-Interface Substructuring FE Model for Reduction of Structural–Acoustic Problems With Poroelastic Damping," Comput. Struct., **89**(23-24), pp. 2233–2248.

[23] Reddy, J., 2004, *Mechanics of Laminated Composite Plates and Shells: Theory and Analysis*, CRC, Boca Raton, FL.

[24] Ohayon, R., and Soize, C., 1998, *Structural Acoustics and Vibration. Mechanical Models, Variational Formulations and Discretization*, Academic, London.